18th World IMACS / MODSIM Congress, Cairns, Australia 13-17 July 2009
http://mssanz.org.au/modsim09

Multiple hydrological stable states and the probability of climate variability causing a threshold crossing

Peterson, T. J. [1], **A. W. Western** [1], **R. M. Argent** [2]

[1] *Department of Civil and Environmental Engineering, The University of Melbourne, Parkville, Australia*
[2] *Water Division, Bureau of Meteorology, Melbourne, Australia*
Email: peterson.tim.j@gmail.com *or* t.peterson@civenv.unimelb.edu.au

Abstract: Many physically based models of surface and groundwater hydrology are constructed without the possibility of multiple stable states for the same parameter set because they do not include positive feedbacks. For such a conceptualisation, at the cessation of a transient hydrological disturbance of any magnitude the model will return to the initial stable state, and thus show an infinite resilience. To highlight and challenge this assumption a numerical distributed eco-hydrological model (coupled hillslope Boussinesq-vertically lumped vadose zone) was developed in which qualitatively different steady state water table elevation and stream flow exist for the same parameter set. It is used herein to quantify catchment resilience to climatic disturbances.

Resilience investigations have traditionally used equilibrium or limit cycle continuation analysis to quantify resilience by estimating the state space location and number of stable states (henceforth referred to as attractors) and thresholds (henceforth referred to as *repellor*). This method requires the use of constant or stable and smooth inter-annual cycles of climate forcing. As groundwater recharge is often dominated by episodic climate events, it is an open question as to whether the multiple hydrological attractors identified from continuation analysis still exist under stochastic climate forcing. Using the above model, this was investigated by undertaking simulations with 100 stochastic climate replicates of 118 years for a range of saturated hydraulic conductivity ($k_{s^{max}}$) parameter values. It allowed assessment of which parameter values: i) lead to bimodal water table elevations emerging, indicating multiple attractors; and ii) quantification of the probability of a shift from a shallow to a deep water table attractor, and vice versa.

To assess bimodal behaviour, for each $k_{s^{max}}$ value the mean depth to the water table over the final year of simulation was calculated and a histogram derived from the 100 simulations. Multiple water table depth attractors (see below) and modes did emerge but were dependent upon the spatially-averaged limiting infiltration rate parameter, I_o. For I_o of 20 mm/day (and $k_{s^{max}}$ from 0.05 to 0.7 m/day) the system shifts from the deep to shallow attractor at the first major rainfall event, thus resulting in only one clear mode. Reducing I_o by 50% and 75% resulted in increasingly clear bimodal water table elevations. The probability of an attractor shift was also calculated and found to be very dependent upon whether the initial state was the shallow or deep water table attractor, with a shift from the deep to the shallow attractor being more probable than the reverse. Overall, this work: i) strengthens the important theory of multiple hydrological attractors; ii) expands quantitative resilience concepts and methods to better incorporate disturbances; and iii) extends characterisation of which catchments are likely to have multiple attractors.

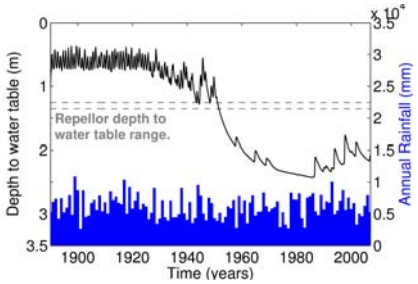

a) Water table, as depth, crossing form the shallow to deep attractor (black line) & annual rainfall (bars).

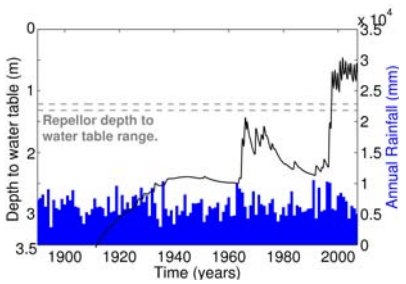

b) Water table, as depth, crossing form the deep to shallow attractor (black line) & annual rainfall (bars).

Keywords: surface-groundwater interactions, quantitative resilience, steady states, stochastic hydrology.

1. INTRODUCTION

Many physically based models of surface and groundwater hydrology are constructed without the possibility of multiple stable states for the same parameter set because they do not include positive feedbacks. For such a conceptualisation, at the cessation of a transient hydrological disturbance of any magnitude the model will return to the initial stable state, and thus show an infinite resilience. To highlight and challenge this assumption Peterson *et al.* (2009) developed a numerical distributed eco-hydrological model (coupled hillslope Boussinesq-vertically lumped vadose zone) in which qualitatively different steady state water table elevation and stream flow exist for the same parameter set. Quantitative resilience investigations attempt to quantify the state space location of such steady states (hence forth referred to as *attractors*) using equilibrium or limit cycle continuation. If forcing data is input to the model, as per most hydrological applications, then continuation analysis requires it to be constant or of stable and smooth cycles (see Peterson *et al.*, 2009 for further details). As stochastic climatic forcing cannot be input, soil moisture is most likely dampened and potentially results in reduced peak unsaturated vertical soil moisture conductivity and reduced groundwater recharge. As the proposed multiple attractors of Peterson *et al.* (2009) are very dependent upon recharge estimates it is thus an open question as to whether they still exist under stochastic climate forcing. For example D'Odorico *et al.* (2005) demonstrated numerically that climate fluctuations can change a soil moisture-vegetation model with two attractors to having only one intermediate attractor. This paper adopts Peterson *et al.* (2009) and undertakes simulations using 100 climate replicates to: i) investigate whether multiple attractors still emerge; and ii) quantify the probability of a shift from a shallow to a deep water table attractor, and vice versa.

2. METHODS

The investigation of multiple water table elevation modes was based on the hillslope Boussinesq–lumped unsaturated zone model of Peterson *et al.* (2009) and, to facilitate comparison, used the parameters, structure, time-step, and monthly average climate forcing of that study. One hundred replicates were derived from daily precipitation and estimated FAO56 ET_o. Simulations were then undertaken for each replicate, the observed climate and the monthly average climate. This was repeated for a range of saturated conductivity parameter values, as per Peterson *et al.* (2009). Trials found that the emergence of multiple attractors was largely dependent upon the limiting infiltration rate parameter and simulations were accordingly also undertaken for three such values. Additional details are given below.

2.1. Surface-groundwater model

As per Peterson *et al.* (2009) the hillslope Boussinesq–lumped unsaturated zone model was parameterised to be of a water supply-limited catchment, land use of grazed pastures with winter-spring dominant LAI, and soil water parameters for sandy clay (Rawls *et al.*, 1982). As per Peterson *et al.* (2009) monthly forcing data was adopted. The boundary condition at the bottom of the catchment was a general head boundary, which simulated interaction with a stream of fixed stage, and at the top a no-flow boundary condition was used.

2.2. Climate Data and Replicates

Daily precipitation and estimated daily FAO56 reference crop evapotranspiration (ET_o) data was obtained from SILO (Jeffery *et al.*, 2001) for a point at 143.45 degrees longitude and -37.10 degrees latitude from 1890 to 2007. These coordinates approximate the daily precipitation gauge 081000 at Avoca (Vic), which is from 1884 to the present, and thus the SILO data strongly resemble observed precipitation. The average annual precipitation and ETo is 542 and 1103 mm/year respectively. The average precipitation to Eto ratio is 0.49 and average annual excess precipitation is 98 mm/year. Figure 1 shows box-plots detailing the distribution of monthly precipitation and evaporation. One hundred 118 year climate replicates were derived using *The Stochastic Climate Library* single site daily climate algorithm (Srikanthan *et al.*, 2004) and the SILO data from 1890 to 2007 inclusively.

2.3. Simulation Experiments

If a water table has only one attractor then irrespective of the initial head or magnitude of disturbance, it will eventually approach this attractor. To investigate the potential for two attractors the model was solved with an initial head of 20% and 98% of the maximum saturated thickness. For specified values of $k_{s^{max}}$ and I_o and each climate replicate, simulations were undertaken from both initial conditions. Simulations were from years 1890 to 2007 inclusive. An alternative to initial conditions at extremes in the maximum saturated

thickness would have been to adopt the state space location of attractors identified from limit cycle continuation in Peterson *et al.* (2009). This was not adopted as it would have increased the number of variables (i.e. scientific variables, not equation variables) in the comparison with results using average climate data (from Peterson *et al.*, 2009) and unnecessarily pre-supposed the attractors identified still emerged using stochastic climate data. For each climate replicate and the two initial conditions, simulations were undertaken at twenty values of $k_{s^{max}}$ (increments of 0.05 m/day from 0.05 to 1.0), each repeated for three values of I_o (5, 10 and 20 mm/day). Thus, 12,000 simulations were performed using a 96 2.4 GHz Xeon processor cluster.

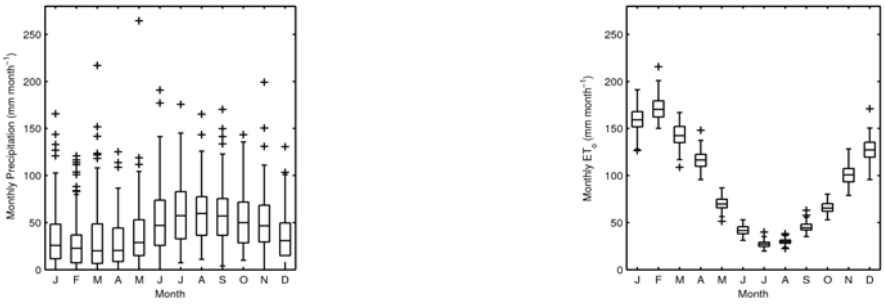

a) Monthly Precipitation. **b)** Potential evaporation (FAO56 ET_o).

Figure 1. *Box-plot of monthly precipitation and ET_o from SILO data (1890 to 2007) at 143.45 degrees longitude and -37.10 degrees latitude.*

The simulation results were analysed for: i) bimodal water table elevation, and ii) the probability of crossing from the deep water table attractor to the shallow attractor and vice versa. For the bimodal investigation, the average water table elevation in the final year of each simulation at 250 metres from the outlet was calculated and, for a given parameter set and initial condition, a histogram of water table elevation produced. The averaging was required to reduce *noise* (from the stochastic climate forcing) in the histograms. A statistical test for bimodality was then undertaken. Investigating the probability of crossing the repellor was more complex. Over the 118 years simulation the water table can, theoretically, repeatedly cross the repellor. Inspection of time-series of heads also found that spurious repellor crossings did occur in which the head slightly crosses and returns again within 1-2 months. Such crossings where not felt to constitute a clear and persistent change in the basin of attraction. As such, the time-series of water table heads were first smoothed using a 24 month moving average. For each smoothed time-series, the number of repellor crossings was then counted. If odd, the simulation was recorded as having a change in the basin of attraction by the final month of simulation. No even number of repellor crossings were detected, thus indicating no simulation crossed the repellor and then returned to the initial basin of attraction. For each parameter set and initial condition, the probability of such a change in the basin of attraction was then estimated by analysing all 100 replicates.

3. RESULTS

3.1. Bi-modal Water Table Elevation

Figures 2 and 3 present the histograms of mean depth to water table when starting from the shallow and deep initial conditions respectively. Each figure presents histograms for three values of saturated conductivity, $k_{s^{max}}$, and repeated for three values of the limiting infiltration rate, I_o. The values of $k_{s^{max}}$ approximates points at 10%, 50% and 90% of the $k_{s^{max}}$ parameter range over which two attractors exist as derived by continuation analysis (Peterson *et al.*, 2009). For a shallow initial water table, Figure 2 illustrates the average water table depth in the final year has a high probability of also being shallow for all nine parameter combinations. Only one mode emerges in each of the nine histograms, thus indicating a very low probability of crossing the repellor into the deep water table attractor. The distributions do though become increasing positively skewed as the $k_{s^{max}}$ percentile increases. Interestingly, the difference between the mode and the depth to water table from the average monthly climatic forcing increases as the $k_{s^{max}}$ percentile increases. For an initially deep water table, Figure 3 illustrates more complex results. For I_o of 10 and 20 mm/day, the water table has a very high probability of crossing the repellor and entering the basin of the shallow attractor, resulting in distributions very comparable to those of Figure 2. For I_o of 5 mm/day each histogram has two clear modes, approximately at the shallow and deep attractors (as indicated by of the blue circles). In summary, two modes, and thus two attractors, can emerge with stochastic forcing but it is very dependent upon the climatic variability and the limiting infiltration rate.

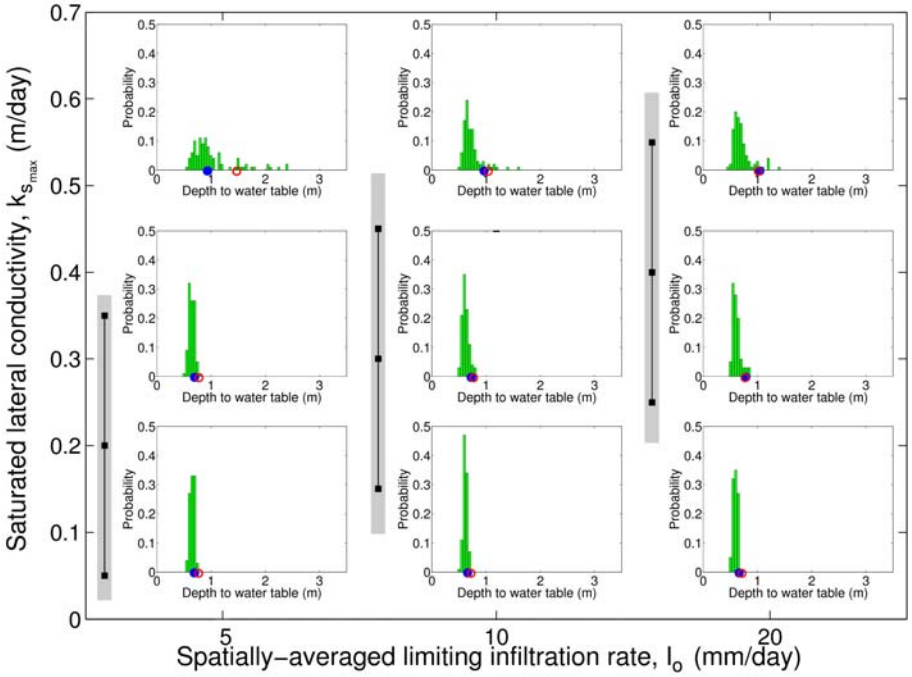

Figure 2. *Histograms of mean depth to water table (green bars) in final year of simulation for the* ***shallow*** *initial water table depth. No histogram has two clear modes. Each column of histograms is of an equal value of I_o, as given by the lower x-axis. Each row is of a different percentage value of the $k_{s_{max}}$ attractor range. The top, middle and bottom rows are at 90%, 50% and 10% the range of two attractors respectively. The range of two attractors was derived using limit cycle continuation (see Peterson et al., 2009). This range is given by the grey vertical bars and the small black squares note the $k_{s_{max}}$ value of the corresponding histogram. The open red circle and blue circle denote the final average depth to water table using the SILO data and monthly average climate data respectively.*

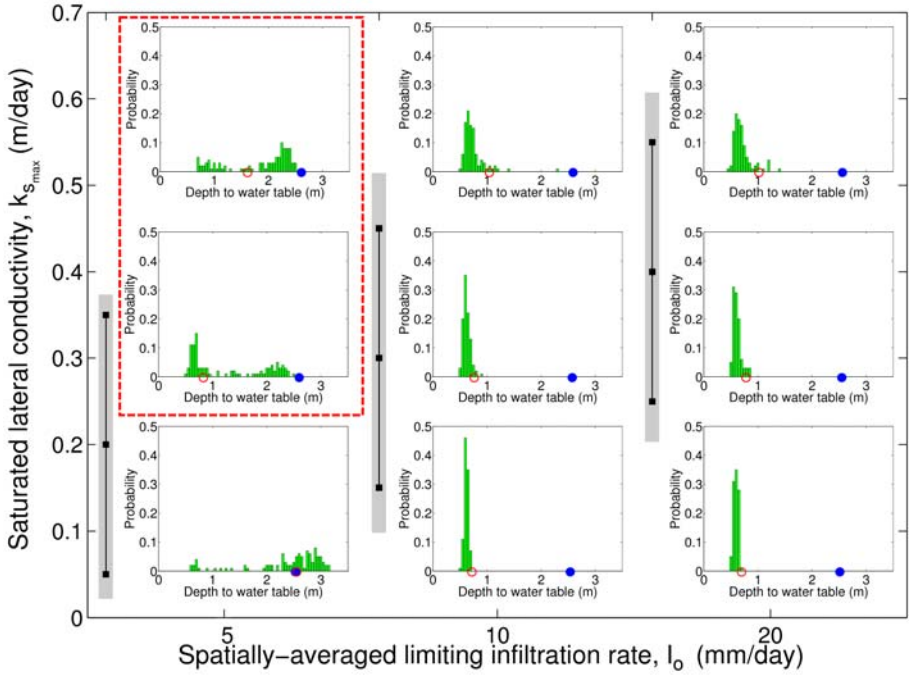

Figure 3. *Histograms of mean depth to water table (green bars) in final year of simulation for the* ***deep*** *initial water table depth. The red dashed box indicates histograms of two clear modes. Additional annotations are as per Figure 2.*

For I_o of 5 mm/day and for both initial conditions, stochastic simulations were also conducted at above and below the $k_{s_{max}}$ range of two attractors. The depth to water table histograms were no longer bimodal, as occurred with the two attractor range, and all of a lower standard deviation. This indicates that continuation

analysis does correctly quantify the range of two attractors and the emergence of bimodal water table elevations is constrained to this range.

The identification of two modes in Figure 3 was somewhat subjective in that no statistical measure was adopted. While no consensus exists for statistical tests of bimodality (Knapp 2007), that of Hartigan and Hartigan (1985) and Hartigan (1985) provides a quantification of the *dip* between modes and the statistical probability the observed modes could emerge from random sampling from a uniform distribution. Specifically, the dip statistic is *'the maximum difference between the empirical distribution function and the unimodal distribution function that minimises that maximum difference'* (Hartigan 1985). It ranges from zero when unimodal to a maximum of 0.25. Table 2.1 presents the dip and significance value, *p*, for each of the nine histograms of Figures 2 and 3. It shows statistically significant (at $p<=0.1$) multiple modes were detected for the deep initial depth when I_o equals 5 mm/day and at the 90% and 50% k_{smax} range (i.e. 0.35 m/day and k_{smax} 0.2 m/day respectively).

Percentile k_{smax} range of two attractors	Shallow Initial Water Table depth			Deep Initial Water Table depth		
	Spatially-averaged limiting infiltration rate, I_o (mm/day)			Spatially-averaged limiting infiltration rate, I_o (mm/day)		
	5	10	20	5	10	20
90%	dip=0.0282 p=*0.8615*	0.0227 *0.9915*	0.0242 *0.9710*	**0.0583** ***0.0100***	0.0198 *0.9980*	0.0242 *0.9805*
50%	0.0349 *0.5325*	0.0319 *0.6890*	0.0250 *0.9580*	**0.0835** ***0.0000***	0.0256 *0.9575*	0.0249 *0.9650*
10%	0.0418 *0.2275*	0.0365 *0.4565*	0.0409 *0.2485*	0.0361 *0.4705*	0.0356 *0.5080*	0.0418 *0.2335*

Table 1: *Bimodal statistical test results using Hartigan (1985). Data from each of the nine histograms of Figures 2 and 3 were tested and are summarised above. The first statistic for a k_{smax} and I_o combination is the dip statistic, a measure of the strength of the dip between two modes. The lower is the statistical significance of the two modes. Two modes of statistical significance were detected (bold) only when the water table was initially at the deeper water table attractor and I_o=5mm/day and k_{smax} = 0.35 and 0.2 m/day (i.e. 90% and 50% percentiles of two attractor range).*

The value of I_o at which two modes emerge is low; however the actual simulated infiltration can significantly exceed 5 mm/day. The parameter, I_o, can be considered as the effective saturated hydraulic conductivity at the surface (Tuteja *et al.*, 2004). At each time step the spatially-averaged potential infiltration rate, I_P, is estimated from the soil moisture deficit and I_o. As a result of sorption, I_P can be greater than I_o. If precipitation is greater than I_P then the resulting infiltration can be greater then I_o. Figure 4 presents the infiltration, for I_o of 5 mm/day, as a function of effective precipitation at six values of soil moisture fraction. For an effective precipitation of above 6 to 10 mm/day, infiltration exceeds the spatially-averaged limiting infiltration rate of 5 mm/day to approach a maximum of 13 mm/day. Thus, the emergence of bimodal water table elevations is not limited to as low an infiltration as suggested by an I_o of 5 mm/day.

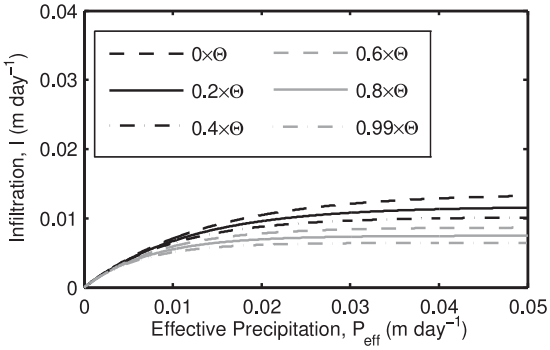

Figure 4. *Infiltration as function of precipitation for I_o= 5mm/day at six values of soil moisture fraction (Θ).*

To highlight the crossing of the repellor, Figure 5 presents time series from two replicates for which the water table crosses from the shallow to the deep attractor and vice versa. Figures 5a shows the water table crossing from the shallow basin of attraction to the deep attractor in 1951 and stabilising around the deep attractor henceforth. Notably, the repellor crossing occurred following a period of only slightly lower rainfall. Figure 5c shows the change to the deep water table attractor basin decreases the streamflow and the baseflow almost ceases. The cessation of the baseflow is due to the fixed stream stage height boundary condition. The LAI is also shown in Figure 5e to increase by approximately one order of magnitude following the crossing to the deep attractor. Figures 5b shows the water table stable around the deep attractor then crossing to the shallow attractor in 1997. Figure 5d shows that baseflow occurs only when the water table is near to or above the repellor and total streamflow increases following the crossing. Figures 5f shows the LAI to decrease by approximately one order of magnitude following the crossing to the shallow attractor.

a) Shallow to deep water table attractor crossing (black lines) and annual rainfall (blue bars).

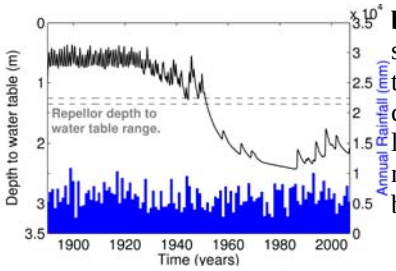

b) Deep to shallow water table attractor crossing (black lines) and annual rainfall (blue bars).

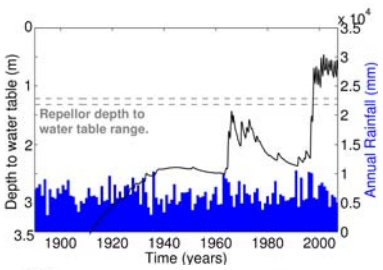

c) Annual stream flow for simulation from *a)* above**.**

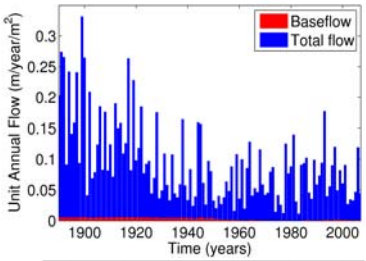

d) Annual stream flow for simulation from *b)* above**.**

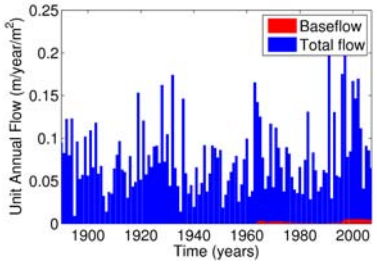

e) Leaf area index for simulation from *a)* above.

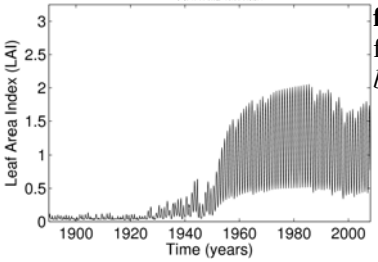

f) Leaf area index for simulation from *b)* above.

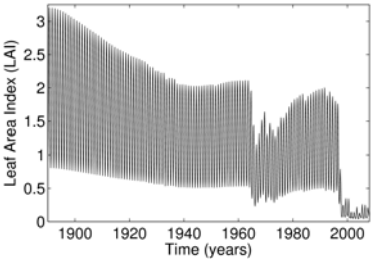

Figure 5. *Time series of depth to water table, streamflow and LAI from a replicate crossing from the shallow to the deep attractor (left column) and vice versa (right column) when I_o=5mm/day and k_{smax}=0.35m/day.*

3.2. Probability of Repellor Crossings

Figure 6 estimates the probability of ending in the alternate basin of attraction from that of the initial conditions after 118 years simulation at the three values of I_o. For the shallow initial attractor there is near zero probability of crossing to the deep basin of attraction, except at the upper k_{smax} limit of the two attractor range (grey rectangle). Conversely, for the deep initial attractor with I_o of 10 and 20 mm/day, the probability of crossing to the shallow basin of attraction approaches 1.0 for k_{smax} in the two attractor range. If though k_{smax} is greater than this range, then the water table will revert to the deep level. For I_o of 5 mm/day there is a significant probability of remaining in the deep basin of attractor whilst in the k_{smax} two attractor range.

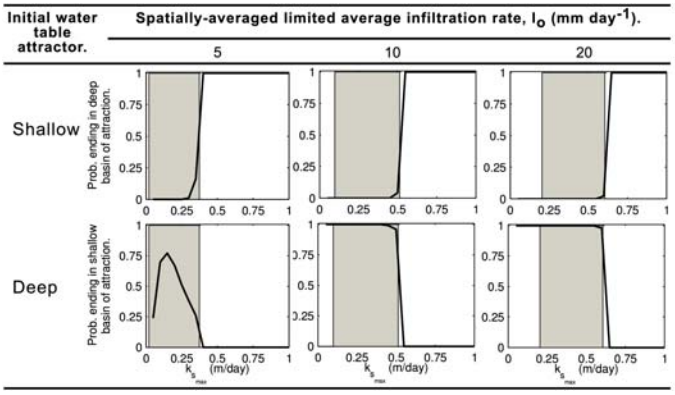

Figure 6. *Probability switching to the alternate basin of attraction after 118 years simulation at the three values of I_o. The shaded rectangle is the k_{smax} range over which two attractors exist.*

4. DISCUSSION AND CONCLUSIONS

The above results demonstrate that duel water table attractors identified by Peterson *et al.* (2009) can emerge under stochastic climate forcing. However their existence was dependent upon the infiltration parameter I_o, such that the two attractors emerged only when I_o equalled 5 mm/day (Figures 2, 3 and Table 1). For I_o of 10

and 20 mm/day, infiltration during the first high rainfall period is sufficient to shift the water table from the deep to shallow basin of attraction. For I_o of 5 mm/day the probability of crossing to the alternate basin of attraction (Figure 6) was asymmetric such that there is a much higher probability of crossing from the deep to the shallow basin of attraction than vice versa. This implies that a less extreme climatic fluctuation is required to cross into the shallow water table attractor than to cross to the deep attractor. Importantly, the asymmetric probabilities are not due to differences in the width of the basin of attraction (i.e. absolute difference in the depth to water table at an attractor from that of the repellor) as derived from continuation analysis. For example, at I_o of 5 mm/day and $k_{s^{max}}$ of 0.25 m/day each attraction is of an equal depth to water table 'distance' to the repellor (0.9 metres depth to water table) but the probability of shifting from the shallow to deep attractor and vice versa are 0% and 50% respectively. The probability plots thus demonstrate deficiencies of continuation analysis, which is a widely used tool for quantifying resilience, and suggests caution in the interpretation of its results. Notably, continuation analysis may predict the location of attractors which are very unlikely to emerge. This is most likely due to it omitting quantification of the basin *resistance*, which is a measure of the 'depth' of the basin (see Walker *et al.*, 2004 for a useful schematic). Inclusion of resistance would most likely identify the deep water table attractor as significantly 'shallower' than the alternate attractor, thus supporting the above identified asymmetric probabilities.

The time series of LAI in Figures 5e and f show that at each of the two water table attractors the LAI differs by at least one order of magnitude. A valid question is whether the two attractors emerge only because of the obvious fact that two different landcovers producing different recharge rates result in different water table elevations. The causal pathway for this question, and many landcover-groundwater investigations, is of a vegetation change (which is almost always assumed anthropogenic) driving the change in the water table elevation. The above attractors emerge though because of the reverse pathway. That is, a change in water table elevation drives a change in landcover (i.e. LAI). If a water table disturbance is sufficient to produce a change to the LAI then a positive feedback can be initiated causing an amplification of the disturbance, resulting in a significant change in the LAI and new equilibrium water table elevation. If the traditional pathway of landcover change driving changes in the water table were adopted then such complex disturbance-response behaviour would be omitted, only one attractor could exist and the system would be of infinite resilience to disturbances. In order for multiple attractors to emerge a positive biophysical feedback is required. Our proposed vegetation-water table positive feedback is unlikely to be the only positive feedback within hydrology. Ongoing development of this and additional positive hydrological feedbacks we hope will raise awareness of the implicit assumption within hydrology of infinite resilience and single stable states and its implications for catchment management.

ACKNOWLEDGEMENTS

The authors are grateful for support from the Australian Research Council (LP04555338), the Murray-Darling Basin Authority and the South Australia Department of Water, Land & Biodiversity Conservation.

REFERENCES

D'Odorico, P., Laio, F. & Ridolfi, L. (2005), Noise-induced stability in dryland plant ecosystems. Proceedings of the National Academy of Sciences of the United States of America, 102(31), 10819-10822.

Hartigan, J. A. & Hatigan, P. M. (1985), The dip test of unimodality, *Annals Of Statistics*, 13(1), 70-84.

Hartigan, P. M. (1985), Computation of the dip statistic to test for unimodality, *Applied Statistics-Journal Of The Royal Statistical Society Series C*, 34, 320-325.

Knapp, T. (2007), Bimodality revisited, *Journal of Modern Applied Statistical Methods*, 6(1), 8-20.

Jeffrey, S.J., Carter, J.O., Moodie, K.M & Beswick, A.R. (2001), Using spatial interpolation to construct a comprehensive archive of Australian climate data, *Enviro. Modelling and Software*, 16(4), 309-330.

Peterson, T.J., R.M. Argent, A.W. Western, and F.H.S. Chiew (2009), Multiple stable states in hydrological models: An ecohydrological investigation, *Water Resour. Res.*, 45, W03406, doi:10.1029/2008WR006886. **http://www.agu.org/pubs/crossref/2009/2008WR006886.shtml**

Rawls, W., Brakensiek, D. & Saxton, K. (1982), Estimation of soil-water properties, *Transactions of the ASAE*, 25(5), 1316–1328.

Srikanthan, S., Chiew, F., & Frost, A. (2007), Stochastic climate library user guide, CRC for Catch. Hydrol.

Tuteja, N.K., Vaze, J., Murphy, B. & Beale G. (2004), CLASS: Catchment scale multiple-landuse atmosphere soil water and solute transport model, Tech. Rep. 04/12, CRC for Catchment Hydrology.

Walker, B., Holling, C.S., Carpenter, S.R., & Kinzig, A. (2004), Resilience, adaptability and transformability in social-ecological systems, *Ecology and Society*, 9(2), 5. **http://www.consecol.org/vol6/iss1/art14/**